

# Uncertainty analysis and robust optimization of multiscale process systems with application to epitaxial thin film growth



Shabnam Rasoulia, Luis Alberto Ricardez-Sandoval\*

Department of Chemical Engineering, University of Waterloo, Waterloo, Canada N2L 3G1

## HIGHLIGHTS

- A method to study model uncertainty propagation in multiscale systems is explored.
- An uncertainty analysis of multiscale systems is conducted using high-order PSEs.
- An efficient tool is developed for robust control of multiscale systems.
- Robust optimization is performed via multiple low-order lattices in KMC simulation.
- Epitaxial thin film growth is used to evaluate the benefit of the present approach.

## ARTICLE INFO

### Article history:

Received 30 January 2014

Received in revised form

26 April 2014

Accepted 5 May 2014

Available online 24 May 2014

### Keywords:

Multiscale modeling

Thin film deposition

Uncertainty analysis

Optimization

Power series expansion

## ABSTRACT

Multiscale modeling of materials growth involves inherently coupled processes that span over a wide range of time and length scales. As a common practice, a multiscale model is adopted to simulate the thin film deposition process that augments Partial Differential Equations (PDEs), describing the macro-scale phenomena, with a high-order lattice-based kinetic Monte Carlo (KMC) simulator, which aims to capture thin film microstructure. Although such a model is a fair representation of the system, the evolution of thin film encompasses processes that are subject to model parameter uncertainty that can significantly affect the control and optimization objectives of this process, e.g. film's roughness and thickness. Thus, to provide a robust and more realistic strategy, it is crucial to perform an uncertainty analysis for this process. This work explores a systematic framework to analyze model parameter uncertainty for robust control and optimization of multiscale models. Such an analysis is extremely challenging due to (i) the lack of a closed formulation between the process optimization objective (i.e. film thickness) and the model parameters and (ii) the computational costs incurred to model the fine-scale events, typically performed using KMC simulation. To tackle these challenges, Power Series Expansion (PSE) is employed to analyze model uncertainty propagation. The PSE-based method for uncertainty analysis is more computationally efficient in comparison to the traditional Monte Carlo approach. The distributional uncertainty in rates of microscopic events is characterized by series expansions of the uncertain parameters. The fitted distributions to the rate of events at a given confidence level are employed to estimate upper and lower bounds on the desired outputs (e.g. film roughness). The computational efficiency of the approach is achieved by employing multiple reduced-order lattices in the KMC simulator. The potential application of the proposed method is illustrated through an optimization problem that aims to specify the robust optimal substrate temperature profile that maximizes the endpoint thin film thickness in the presence of uncertainty.

© 2014 Elsevier Ltd. All rights reserved.

## 1. Introduction

Thin film deposition is an important multiscale process in semiconductor manufacturing which comprises phenomena that evolve at different time and length scales (Vlachos, 2005). Strong

dependence of the electrical and mechanical properties of thin films on their microstructure requires an accurate control of the product quality at the fine scale (Christofides and Armaou, 2006; Christofides et al., 2008; Middlebrooks and Rawlings, 2007). To model the system, the surface evolution during the thin film deposition can be described using KMC simulations (Gilmer and Bennema, 1972). KMC simulation develops the numerical solution to the underlying master equation, which provides the true evolution of the film (Fichthorn and Weinberg, 1991). Such a

\* Corresponding author. Tel.: +1 519 888 4567x38667; fax: +1 519 888 4347.  
E-mail address: [laricard@uwaterloo.ca](mailto:laricard@uwaterloo.ca) (L.A. Ricardez-Sandoval).

simulation, however, is high-dimensional and stochastic in nature, thus limiting its application for optimization and control purposes. Therefore, estimation and control in this process is often accomplished through the application of model reduction techniques for the master equation. Gallivan and Murray (2004) developed a reduced-order model by grouping microscopic configurations with similar overall statistics that evolve together and removing the states that are unlikely to occur (Gallivan, 2005; Gallivan and Murray, 2004). The reduced-order model was later used to estimate the optimal time-varying temperature profile offline (Gallivan, 2003; Gallivan and Atwater, 2004). Nevertheless, detailed modeling of the thin film growth process requires capturing phenomena that occurs over multiple interacting scales. To address this issue, multiscale modeling and analysis has emerged as an attractive approach to improve the predicting capabilities in these systems (Albo et al., 2006; Dollet, 2004; Majumder and Broadbelt, 2006). Vlachos (1997) employed macro-scale continuum equations embedded with micro-scale lattice-based KMC simulations resulting in a multiscale integration hybrid algorithm that simulates homogeneous/heterogeneous processes. To study the effect of macroscopic parameters on the epitaxial growth mode, coupling of the PDE model and KMC is accomplished through the system's boundary conditions (Lam and Vlachos, 2001; Vlachos, 1999). The inherently coupled multiscale model motivates strategies to control film microstructure through the manipulation of macro-scale variables. However, one limitation of the hybrid multiscale models is that they do not provide a closed-form expression due to the use of a stochastic (KMC) model to describe the fine-scale phenomena. Hence, the direct application of these models for online control and optimization is computationally prohibitive. To control these processes, reduction of multiscale systems is performed through proper orthogonal decomposition (Raimondeau and Vlachos, 2000). In (Varshney and Armaou, 2006), the feedback control of thin film microstructure has been achieved via offline identification of a low-order model for a finite set of coarse observable variables. Also, a computationally efficient methodology has been proposed to maximize film uniformity and minimize the roughness in a thin film growth process (Varshney and Armaou, 2005). Lou and Christofides have presented a methodology for real-time estimation and control of roughness and growth rate during thin film deposition using multiple reduced-order lattices in KMC simulations (Lou and Christofides, 2003a, 2003b, 2004). Due to considerable issues associated with feedback control, experimental design has also gained attention to determine the process optimal operating conditions (Prasad and Vlachos, 2008). To perform the identification, the multiscale model can be reduced using clustering or principal component analysis (Subramanian et al., 2011).

Although advances in computer science and optical sensors have resulted into a considerable growth in multiscale modeling and control research during the past decade, this field is still in its elementary stages and correspondingly presents a variety of challenges (Ricardez-Sandoval, 2011; Yang, 2013). In particular, new issues arise due to system's complexity and the coupling of continuum and non-continuum models (Braatz et al., 2004; Rusli et al., 2004; Vlachos, 2012). Fine-scale models often include parameters that are difficult to estimate using experiments or estimates are not known with absolute certainty. Moreover, the lack of knowledge about phenomena occurring at this fine-scale increases the model complexity (Braatz et al., 2006). In process modeling and analysis, the discrepancy between the actual process and the model is expected. The performance of model-based control and optimization techniques can be deteriorated due to inappropriate assumptions applied in the model development and model uncertainty. Specifically, when the system's performance objective is highly sensitive to changes in the system's physical

parameters, this model inaccuracy or mismatch can significantly lead to loss in performance. To design a robust control or optimization framework, it is therefore essential to take model parameter uncertainty into account. As a result, multiscale system tools are required to account for uncertain mechanisms and uncertainty in the model parameters. Despite its importance, uncertainty analysis in multiscale systems has not been widely studied. Nagy and Allgower (2007) have demonstrated the performance of a robust nonlinear model predictive control scheme that takes parameters uncertainty into account in the controller design using the reduced-order model developed by Gallivan for a deposition process. Also, in the context of control of thin film porosity, a model predictive controller was designed to control film porosity to the desired level and reduce its run-to-run variability (Hu et al., 2009). The computational efficiency of predictive control algorithms are achieved through approximation of finite dimensional stochastic PDEs (Ni and Christofides, 2005; Zhang et al., 2010).

Motivated by these observations, the objective of this research is to study model uncertainty propagation in multiscale process systems. The widely used technique for uncertainty propagation is based on the Monte Carlo framework which employs the primary model and a large number of sample points from the uncertain parameters' probability density functions. While this method is promising for many problems, it is computationally intensive especially for online applications. An alternative approach is to employ analytical mathematical tools that are aimed to quantify the impact of parameter and control implementation uncertainties on the systems' performance. The key idea with these methods is to obtain a simpler representation of the actual system using for example Power Series Expansions (PSE) or polynomial chaos expansion to propagate the uncertainty in the system's outputs or states. The resulting analytical expressions are also appropriate for calculating the moments of the process outputs analytically. The implementation of these methods to study uncertainty propagation for macro-scale systems is available in the literature (Ma and Braatz, 2001; Nagy and Braatz, 2003, 2004, 2007). In molecular simulations, on the other hand, PSE is employed to map the key parameters to the simulation outputs (Rusli et al., 2007). Quantitative analysis using first-order PSE, therefore, is performed to identify the most sensitive parameters based on experimental measurements during copper electrodeposition. To efficiently optimize the parameters, the computationally intensive molecular models are approximated using the series expansion of the key parameters (Raimondeau et al., 2003). In those works, PSEs have been employed for sensitivity analysis and model identification in multiscale systems. That is, they have applied PSE to identify low-order models from experimental observations. None of those studies, however, explored robust optimization in multiscale systems under uncertainty.

This paper focuses on uncertainty analysis in multiscale systems for the purpose of robust control and optimization. The proposed method employs PSE, and its effectiveness is evaluated using robust optimization. To describe the uncertainty in a multiscale process, the uncertainty in the rates of microscopic events is characterized using PSE. That is, the expression relating the system's microscopic rates and the uncertain parameters is approximated by a series expansion. This approach is employed to evaluate probabilistic bounds on the desired outputs based on a priori distribution of the uncertain parameters. The systematic uncertainty analysis framework explored in this work to address uncertainty analysis for multiscale systems is tested by performing the robust optimization of a thin film deposition process. The aim in that optimization is to identify the optimal process operating conditions with respect to a cost functional that comply with the process feasibility constraints in the presence of uncertainty in the

multiscale model parameters. To the authors' knowledge, this is the first study that performs robust optimization for multiscale systems.

This paper is organized as follows: Section 2 provides the detailed mathematical expressions for modeling of the thin film growth process as a simple but effective representative of a multiscale process system. The system is modeled linking the continuum conservation laws with KMC simulations that capture the microscopic processes. In Section 3, the PSE-based method to analyse the uncertainty is described. Also, a computationally efficient methodology is proposed to estimate the upper and lower bounds for the process outputs using PSE. In Section 4, the uncertainty analysis technique presented in the previous section is then used to formulate a robust optimization problem that aims to improve the efficiency of a multiscale thin film process under uncertainty. Concluding remarks are presented at the end of this paper.

## 2. Thin film growth model

For many technological applications, high quality films are produced by the process of vapor deposition (Gadgil, 1993). In a typical vapor deposition chamber, the gas flow in the chamber develops a uniform boundary layer adjacent to the surface of the deposition. This uniform boundary layer of width  $\delta$  is shown in Fig. 1. The precursor species from the bulk diffuse through this boundary layer to form a thin solid film. In the present study, an epitaxial thin film growth process in the stagnation point flow chamber is considered. A schematic of this chamber is depicted in Fig. 2, which employs a gas distributor to obviate the substrate rotation. To deal with disparate length and time scales, continuum momentum, energy and mass conservation balances are employed to describe the boundary layer next to the surface of the thin film whereas the evolution of the surface microstructure is captured through KMC simulations (Christofides et al., 2008; Lam and Vlachos, 2001).

### 2.1. Gas phase model: modeling the macro-scale

At the macroscopic level, continuum descriptions of fluid flow, heat and mass transfer for the species that contributes towards the deposition can be described as follows (Sharma and Sirignano, 1969; Song et al., 1991):

$$\frac{\partial}{\partial \tau} \left( \frac{\partial f}{\partial \eta} \right) = \frac{\partial^3 f}{\partial \eta^3} + f \frac{\partial^2 f}{\partial \eta^2} + \frac{1}{2} \left[ \frac{\rho_b}{\rho} - \left( \frac{\partial f}{\partial \eta} \right)^2 \right], \quad (1)$$

$$\frac{\partial T}{\partial \tau} = \frac{1}{Pr} \frac{\partial^2 T}{\partial \eta^2} + f \frac{\partial T}{\partial \eta}, \quad (2)$$

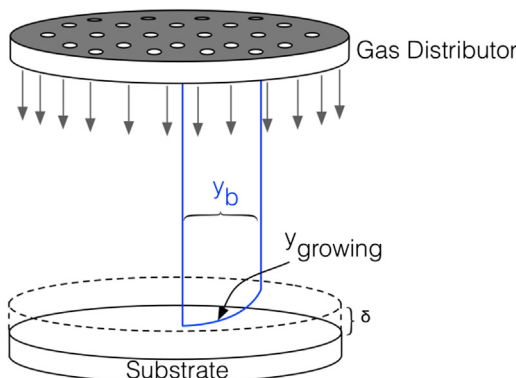


Fig. 1. Schematic of the boundary layer on the substrate.

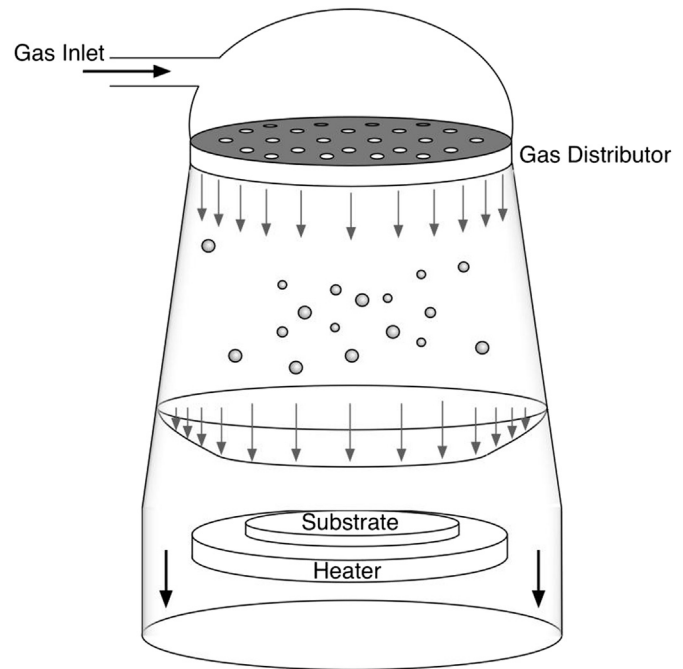


Fig. 2. Schematic of stagnation point flow vapor deposition chamber.

$$\frac{\partial y}{\partial \tau} = \frac{1}{Sc} \frac{\partial^2 y}{\partial \eta^2} + f \frac{\partial y}{\partial \eta}. \quad (3)$$

The boundary conditions for the bulk ( $\eta \rightarrow \infty$ ) are:

$$\begin{aligned} \frac{\partial f}{\partial \eta} &= 1, \\ T &= T_{bulk}, \\ y &= y_b. \end{aligned} \quad (4)$$

Likewise, the boundary conditions on the surface ( $\eta \rightarrow 0$ ) are as follows:

$$\begin{aligned} f &= 0, \\ \frac{\partial f}{\partial \eta} &= 0, \\ T &= T_{surface}, \end{aligned} \quad (5)$$

$$\frac{\partial y}{\partial \eta} = \frac{Sc(R_a - R_d)}{\sqrt{2a\mu_b\rho_b}}. \quad (6)$$

In Eqs. (1)–(6),  $f$  denotes the dimensionless stream function,  $\eta$  is the dimensionless distance to the surface,  $\rho$  is the density of the mixture,  $Pr$  is the Prandtl number,  $y$  and  $Sc$  are the mole fraction and Schmidt number of species, respectively. The parameters  $\mu_b$  and  $\rho_b$  are the viscosity and the density of the bulk, respectively;  $a$  is the hydrodynamic strain rate and  $\tau = 2at$  is the dimensionless time.  $R_a$  and  $R_d$  depend on the rates of adsorption and desorption, respectively. The strong interactions between the microscopic processes occurring at the surface and the gas phase scale processes are accounted for in the boundary condition indicated in Eq. (6).

### 2.2. Surface structure model: modeling the micro-scale

Due to the stochastic nature of the processes taking place on a thin film surface, the probability that the surface is in a particular configuration can be described using the master equation (Van Kampen, 1992)

$$\frac{dP(\sigma, t)}{dt} = \sum_{\sigma'} W(\sigma' \rightarrow \sigma) P(\sigma', t) - \sum_{\sigma'} W(\sigma \rightarrow \sigma') P(\sigma, t), \quad (7)$$

where  $\sigma$  and  $\sigma'$  denote two successive states of the system,  $P(\sigma, t)$  is the probability that the system is in state  $\sigma$  at time  $t$ , and  $W(\sigma \rightarrow \sigma')$  is the probability per unit time that the system will undergo the transition from state  $\sigma$  to state  $\sigma'$ . The master equation results in a system of first-order Ordinary Differential Equations (ODEs); each equation represents the probability of an individual state in the system at certain time  $t$ . While the solution of the master equation can be obtained using traditional numerical methods for solving ODEs, the challenge with this formulation lies on the number of states that need to be evaluated. For systems with even a relatively small size, the master equation cannot be solved since the number of possible states is prohibitively large, e.g., a surface lattice consisting of 100 sites with a maximum height of one has  $2^{100}$  number of configurations. This imposes a limitation towards the direct application of the master equation to obtain an estimate of the system states. The KMC method provides a numerical solution to the underlying master equation (Fichthorn and Weinberg, 1991). A lattice-based KMC can be used as a representative of the underlying structure. In this method, the states of the system are defined by occupancy of lattice sites.

The KMC simulation tool is referred to as a discrete Markov evolution of a system where time increments are obtained via an exponential distribution. In the KMC algorithm, the microscopic rates of all possible processes or events are calculated from the current state of the system. Based on the current probabilities of occurrence of those processes, a process is selected using a random number taken from a uniform distribution. Once the event has been executed in the system, the time is incremented through another random number. Updating the transition probabilities and modifying the configuration appropriately is essential for next step execution. The temporal and spatial changes occurring at the surface are dominated by the microscopic processes. In this work, three microscopic processes contribute towards the development of the thin film: (i) adsorption of particles from the gas phase to the surface, (ii) desorption of particles from the surface to the gas phase, and (iii) migration of particles to an adjacent site on the surface. The surface of a simple cubic lattice is used to describe the thin film growth. In the present multiscale model for thin film epitaxial deposition, the KMC lattice at any time  $t$  is represented as a matrix,  $\mathbf{S}$ , where each element in this matrix represents the number of particles located on each site within the surface lattice, i.e.,

$$S(t) \triangleq \{h(i, j) : i, j = 1 \dots N\} \quad (8)$$

where  $N$  denotes the lattice size and  $h(i, j)$  is the surface height or number of particles at site  $(i, j)$ .

To reduce the computational costs, the method has been implemented for a limited-size lattice assuming periodic boundary conditions. Another assumption is solid-on-solid (SOS) approximation, based on which, overhangs and vacancies are not allowed and particles are located on top of other particles on the surface. Moreover, it is assumed that the interactions between particles have a length of first nearest neighbors.

In this study, it is assumed that all the surface sites are available for adsorption. The total rate of adsorption event on the surface can be determined from the kinetic theory of ideal gases (Lam and Vlachos, 2001)

$$W_a = \frac{S_0 p y_{\text{grow}} N^2}{\sqrt{2\pi m R T C_{\text{tot}}}} \quad (9)$$

where  $S_0$  is the sticking coefficient,  $p$  is the total pressure of gas phase,  $y_{\text{grow}}$  is the mole fraction of precursor on the surface,  $C_{\text{tot}}$  is the concentration of sites on the surface,  $m$  is the precursor molecular weight,  $R$  is the gas constant,  $T$  is the substrate temperature. Macroscopic scale affects the film growth on the

surface through  $W_a$  since estimates for  $y_{\text{grow}}$  are obtained from the solution of the gas phase mass transfer equation shown in Eq. (3).

In the present analysis, desorption and migration events are considered to be site-dependent. The first nearest neighbors assumption results in five classes of surface particles, which can have from one (only a vertical bond) neighbor, up to five (all surface bonds and a vertical bond) neighbors. Therefore, particles in each class have the same probability of desorption and migration since they have the same number of nearest neighbors. In the desorption process, a particle overcomes the energy barrier of the surface and returns to the gas phase. Consequently, the rate of desorption depends on the activation energy and the local environment of the surface. The total rate of desorption event is calculated as follows:

$$W_d = \sum_{i=1}^5 k_{d0} M_i e^{-(iE + E_d)/RT} \quad (10)$$

where  $M_i$  is the number of surface particles with  $i$  nearest neighbors,  $E$  denotes the energy associated with a single bond on the surface,  $E_d$  is the energy associated with desorption and  $k_{d0}$  is an event-frequency constant. Likewise, the total rate of migration is estimated as follows:

$$W_m = \sum_{i=1}^5 k_{d0} M_i e^{-(iE + E_m)/RT} \quad (11)$$

where  $E_m$  is the energy associated with migration.

The resulting rates can then be used to select an event using Monte Carlo sampling methods. That is, a random number generated from a uniform distribution is used to select the next event to be executed on the surface. Then, a second random number is needed to pick the site within the lattice where the event will be executed. Upon successful event execution, the time, which was needed to execute the Monte Carlo event on the surface, is incremented using the following expression:

$$dt = \frac{-\ln \zeta}{W_a + W_d + W_m}, \quad (12)$$

where  $\zeta$  is a uniform random number from a (0,1) interval and  $dt$  is the time increment in the KMC model.

The transport phenomena in the gas phase influence the growth occurring on the surface via the local supply of mass to the surface whereas the microscopic phenomena on the surface affect the overall mass transfer taking place above the surface. That is, the amount of precursor available to deposit on the surface depends on the macroscopic properties of the system. Conversely, the consumption of the precursor on the surface affects the mass flux above the surface. Hence, the macroscopic model and the KMC model depend on each other and are connected through the boundary condition indicated in Eq. (6). The parameter of the adsorption rate at the microscopic scale, i.e., the precursor mole fraction on the surface  $y_{\text{grow}}$ , is provided from the mass transfer balance shown in Eq. (3). In addition, the mass transfer boundary condition at the surface depends on the microscopic processes. As shown in Eq. (6),  $R_a$  and  $R_d$  correspond to adsorption and desorption events; the difference between these values can be obtained as follows:

$$R_a - R_d = \frac{N_a - N_d}{2a N^2 \Delta T}, \quad (13)$$

where  $\Delta T$  is the coupling time instance between the macroscopic and the microscopic simulations.  $N_a$  is the number of adsorbed atoms during  $\Delta T$  and  $N_d$  is the number of desorbed atoms in the same time interval. The values of the parameters used in this study are depicted in Table 1.



**Table 1**  
Model parameters and their corresponding values and units.

Parameter	Symbol	Value
Concentration of sites on the surface	$C_{tot}$	$1.6611 \times 10^{-5}$ sites.mol/m <sup>2</sup>
Energy associated with a single bond	$E$	17 000 cal/mol
Energy associated with desorption	$E_d$	17 000 cal/mol
Energy associated with migration	$E_m$	10 200 cal/mol
Event-frequency constant	$k_{d0}$	$1 \times 10^9$ 1/s
Precursor molecular weight	$m$	0.028 kg/mol
Chamber pressure	$p$	$1 \times 10^5$ Pa
Sticking coefficient	$S_0$	0.1
Strain rate	$a$	5 1/s
Schmidt number of the growing species	$Sc$	0.75
Mole fraction of precursor in the bulk	$y_b$	$2 \times 10^{-6}$
Viscosity of bulk multiplied by its density	$\mu_b \rho_b$	$9 \times 10^{11}$
Ratio of bulk density to thin film density	$\rho_b / \rho$	1

### 2.3. Roughness, growth rate and thickness

High surface roughness can adversely affect the properties of the film and therefore the electronic devices. Accordingly, roughness is a key property that directly determines the quality of a thin film and it can be estimated based on the average number of the broken bonds on the surface (Raimondeau and Vlachos, 2000):

$$r = 1 + \frac{\sum_{ij} (|h_{i+1,j} - h_{i,j}| + |h_{i-1,j} - h_{i,j}| + |h_{i,j+1} - h_{i,j}| + |h_{i,j-1} - h_{i,j}|)}{2N^2}, \quad (14)$$

where  $h_{i,j}$  is the surface height or number of particles at site  $(i,j)$ . Thickness of the thin film at any time during the deposition can be calculated from average of the surface height using the following expression:

$$H = \frac{1}{N^2} \sum_{ij} h_{i,j} \quad (15)$$

Another critical characteristic of the thin film process that needs to be monitored is the growth rate (Middlebrook and Rawlings, 2006). This property determines how fast the thin film grows and therefore affects the process productivity. Growth rate can be determined as follows:

$$Gr = \frac{\sum_{ij} \Delta h_{i,j}}{N^2 \Delta t}, \quad (16)$$

where  $\Delta h_{i,j} = h_{i,j}(t + \Delta t) - h_{i,j}(t)$  is the change in the surface height at site  $(i,j)$  during  $\Delta t$ .  $\Delta t$  is a specific time interval where the growth rate needs to be estimated.

In KMC simulations, the accuracy of the results relies on the lattice size used to simulate the evolution of the thin film. Since KMC is a stochastic realization of the so-called master equation, large lattice sizes produce results that converge to the solution of the master equation. Nevertheless, the simulation of large lattice sizes is computationally expensive. Thus, there is a trade-off between accuracy in the system outputs and computational cost. In Fig. 3, the evolution of the surface roughness at  $T=800$  K is demonstrated from KMC simulators that use  $150 \times 150$  and  $100 \times 100$  lattices. The accuracy of the results is not significantly improved when using a  $150 \times 150$  surface lattice. The computational time required to simulate the growth process are also indicated in Table 2 for different lattice sizes in the KMC simulation. The KMC simulation using a  $100 \times 100$  lattice provides a good approximation of the process with relatively low computational costs. Accordingly, in the current study, a  $100 \times 100$  surface lattice is used to represent the actual thin film epitaxial deposition process.

To implement an online scheme for the surface roughness, the size of the lattice has to be selected in such a way that the computational time needed to obtain an estimate of the surface properties be comparable to the process real-time evolution. In these simulations, when the lattice size is reduced to  $N=30$ , it captures the evolution of the surface roughness and growth rate with reasonable computational efficiency. As depicted in Fig. 4, the result obtained from reduced-order lattice simulation contains significant fluctuations in comparison to the simulation which uses a  $100 \times 100$  lattice; however, the overall transient evolution of the surface is captured by the  $30 \times 30$  surface lattice. To circumvent the issue of fluctuations, similar to the approach presented in (Lou and Christofides, 2003) the roughness values obtained from multiple independent reduced-order KMC simulations using the same parameters can be averaged. Fig. 4 shows that the roughness estimated from averaging six  $30 \times 30$  lattices provides a good representation of the actual process, i.e., a  $100 \times 100$  KMC-lattice model. According to Fig. 4 and Table 2, averaging six  $30 \times 30$  lattices provides accurate results at low computational costs.

### 3. Probabilistic bounds using power series expansion

The present analysis assumes that the multiscale model described in the previous section is available for simulations. In PSE-based methods, the uncertainty quantification is performed through the approximation of the nonlinear dynamic behaviour of the system using a series expansion. Taking advantage of a prior knowledge about the distribution of the uncertain parameters, a distributional uncertainty analysis of the states and outputs can be performed. Another key advantage of this approach is that it is not necessary to have the analytical expression for the function since it only requires the function sensitivities with respect to the uncertain parameters. Following this approach; the issue of absence of closed-form models can then be addressed by deriving a low-order model. The variability in states and outputs of finite-time processes is mostly assessed using first-order series expansion. Accurate estimates of the variability, however, can be obtained by adding more terms to the PSE (Ma and Braatz, 2001; Nagy and Braatz, 2003).

The difficulty in multiscale sensitivity analysis is the inherent noise included in the system's response due to stochastic (KMC) model used to describe the fine-scale events in the epitaxial deposition process described above. Drews and coworkers have analysed the sensitivity of the model parameters involved in a multiscale Monte Carlo simulation code using finite differences formulated as a stochastic optimization (Drews et al., 2003). They

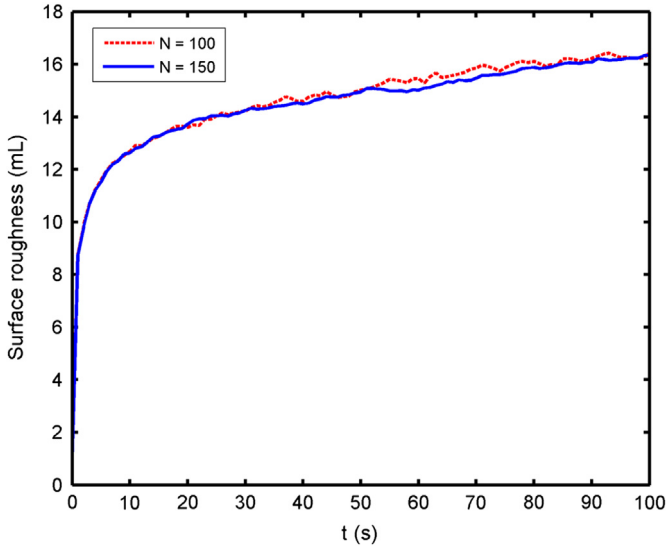


Fig. 3. Comparison of the surface roughness evolution obtained from different simulations using  $150 \times 150$  and  $100 \times 100$  lattices.

**Table 2**  
Computational cost of various lattice sizes employed in the KMC simulation.

Lattice size	Computational time (s)
$N = 150$	2448
$N = 100$	747
$N = 30$	47
Average of six $N = 30$	135

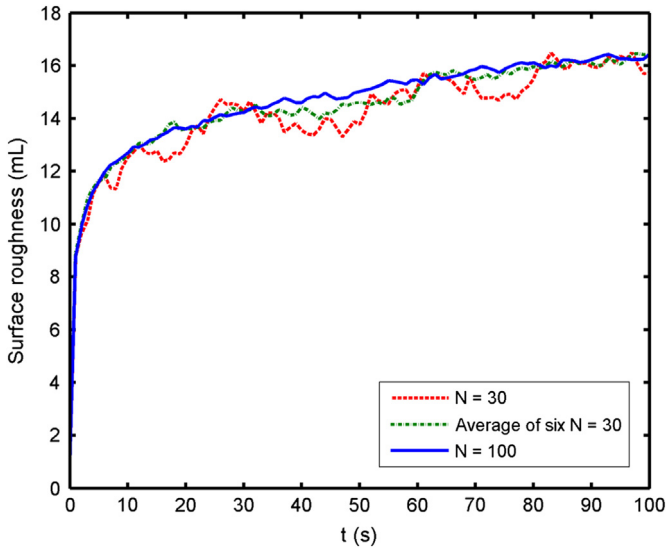


Fig. 4. Comparison of the surface roughness evolution obtained from different simulations using  $100 \times 100$ ,  $30 \times 30$  lattices and average of six  $30 \times 30$  lattices.

utilized Condor, a high throughput computing environment, to perform this computationally intense investigation. Due to issues associated with the sensitivity analysis of outputs with respect to the uncertain parameters, in the current work, the uncertainty propagation is performed for the rate of the microscopic events. Estimation of the distribution of these rates using the PSE-based approach is not sufficient for execution of KMC events. Accordingly, once the distributions are obtained, specific values can be selected based on a predefined confidence level. The detailed

description of the proposed framework to address the uncertainty analysis for multiscale systems is described next.

### 3.1. Uncertainty propagation using PSE

Define the vector of uncertain parameters  $\theta = \{\theta_1, \dots, \theta_q, \dots, \theta_Q\} \in \mathbb{R}^Q$ ,  $\hat{\theta}$  as the vector of nominal model parameters and the microscopic rates vector  $\mathbf{W} = \{W_1, \dots, W_n, \dots, W_N\} \in \mathbb{R}^N$ , the algorithm to obtain the distributional uncertainty of rates of microscopic events at any time during the process can be outlined as follows:

1. Specify the prior probability distribution function of each uncertain parameter,  $f_{p,d}(\theta_q)$ .

$$\theta_q = \{\theta_q | \theta_q \in f_{p,d}(\theta_q)\} \quad (17)$$

2. Evaluate the sensitivities of rate of each of the microscopic events with respect to the uncertain parameters using the multiscale model at a specific time  $t$ . The order of the required sensitivities relies on the order of PSE. For instance, the first and second-order sensitivities are as follows:

$$\mathbf{L}_1(t) = \left( \frac{\partial \mathbf{W}}{\partial \theta} \right)_{\theta = \hat{\theta}}, \mathbf{L}_2(t) = \left( \frac{\partial^2 \mathbf{W}}{\partial \theta^2} \right)_{\theta = \hat{\theta}} \quad (18)$$

3. Estimate the probability distribution function of  $W_n$  using the following truncated power series expansion:

$$W_n = \hat{W}_n + \mathbf{L}_1(\theta - \hat{\theta}) + \frac{1}{2}(\theta - \hat{\theta})^T \mathbf{L}_2(\theta - \hat{\theta}) + \dots, \quad (19)$$

where  $\hat{W}_n$  is the nominal microscopic event rate. The probability distribution function for  $W_n$  can be obtained by solving (19) for different Monte Carlo realizations in  $\theta$  that comply with the prior distribution assigned to each of the uncertain parameters. The order of the PSE depends on the nonlinearity of the function and the variability of the uncertain parameter. To determine the order of the expansion, the results have to be compared with brute-force Monte Carlo simulation that uses the primary model. The order of the expansion has to be increased until the approximation is accurate enough.

4. Estimate the upper and lower bounds on  $W_n$  at a predefined confidence level,  $\alpha$ .

$$W_n^k = F^{-1}(P | W_n) = \{W_n : F(W_n)\} \quad (20)$$

where  $k \in \{low, up\}$  and the function  $F^{-1}(P | W_n)$  represents the inverse of cumulative distribution function evaluated at a predefined probability,  $P$ . Setting  $P$  in Eq. (20) to  $\alpha/2$  and  $1 - \alpha/2$  yields respectively the lower bound,  $W_n^{low}$ , and the upper bound,  $W_n^{up}$ , for the  $n^{th}$  event rate,  $W_n$ .

In order to investigate the accuracy of the proposed framework, a comparison between the probability distributions of rate of adsorption obtained using the primary model and the PSE-based method was performed. The uncertainty analysis was performed with respect to the bulk mole fraction,  $y_b$  which according to the multiscale model presented in Section 2 is the boundary condition of the mass transfer equation shown in Eq. (4). This parameter has a significant effect on the total rate of adsorption ( $W_a$ ) and therefore on the overall multiscale model. To that end, after a finite time interval in the open-loop simulation, the distributions of the total adsorption rate were obtained from Monte Carlo simulations using the primary model and the PSE-based model, obtained from the method described above. As it was previously mentioned, the Monte Carlo method requires a large number of samples from the uncertain parameter distribution. Particularly for

this system, more than 500 data points have to be generated to obtain a representative distribution for the total rate of adsorption while using the primary multiscale model. To study the effect of uncertainty in the bulk mole fraction, random numbers are generated from a normal distribution with mean  $2 \times 10^{-6}$  and standard deviation  $2 \times 10^{-7}$ . Employing these data points, the uncertainty is propagated into the total adsorption rate using the multiscale model presented in Section 2 at  $T=800$  K. The histogram obtained at  $t=10$  s is presented in Fig. 5. The variability is also assessed using a first-order PSE and the fitted normal distribution is shown in Fig. 5. As depicted in this figure, the distribution obtained from the PSE-based model accurately describes the variability in the total rate of adsorption due to the uncertainty in  $y_b$ . The required computational times are indicated in Table 3. As shown in that table, the Monte Carlo method is at least two orders of magnitude more intensive than the PSE-based method, which is the key benefit of the present approach. Using the distribution obtained for total rate of adsorption, then upper and lower bounds for the adsorption rate at the current time  $t$ , i.e.,  $W_a^{low}(t)$ ,  $W_a^{up}(t)$ , can be estimated at a given confidence level ( $\alpha$ ). The corresponding values at  $\alpha=1\%$  are shown in Table 3.

Though the first-order series expansion is appropriate for the bulk mole fraction, it is not sufficient to propagate the uncertainty in other system's parameters, e.g.,  $E$  and  $E_m$ . As shown in Eqs. (10) and (11), the energy associated with a single bond and migration affect the microstructure through a nonlinear Arrhenius-type expression of desorption and migration probabilities. In this case, the PSE needs to be derived using higher order terms due to the existence of non-linearity between the uncertain parameters and the microscopic events. Therefore, second-order PSE is applied to study the uncertainty propagation in total rate of desorption and migration due to variability in these parameters. To study the effect of the variability in the adsorption, migration and desorption rates, uncertainty in  $y_b$ ,  $E$  and  $E_m$ , was considered in the analysis. The uncertainty considered for  $y_b$  was

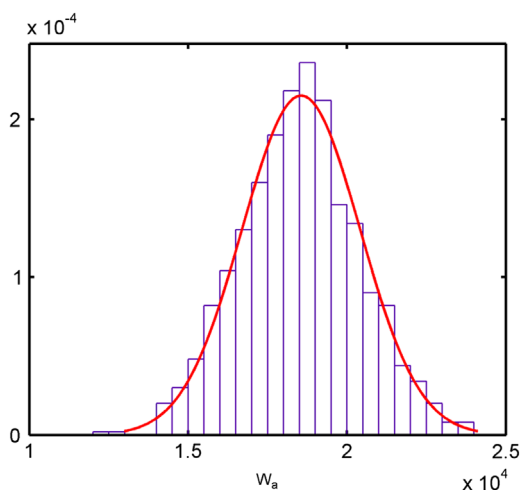


Fig. 5. Probability distribution function of the total adsorption rate from Monte Carlo applied to primary model using 500 points and the distribution obtained using first-order PSE.

Table 3

The probabilistic bounds of the total rate of adsorption from different approaches at  $t=10$  s and the corresponding computational cost.

Approach	$W_a^{low}(1/s)$	$W_a^{up}(1/s)$	Computational time (s)
Monte Carlo using the primary model	$1.41 \times 10^4$	$2.33 \times 10^4$	34980
1 <sup>st</sup> -order PSE	$1.38 \times 10^4$	$2.34 \times 10^4$	390

similar to that described above, i.e.,  $\mathcal{N}(2 \times 10^{-6}, 2 \times 10^{-7})$  while  $E$  and  $E_m$  were also assumed to follow normal distributions around their nominal values,  $[\hat{E}, \hat{E}_m] = [17\,000, 10\,200]$ , with the standard deviation of 500. The probability distribution functions obtained using PSE-based model for the microscopic events at different times are shown in Fig. 6.

### 3.1. Computation of the probabilistic-based bounds

The algorithm described above to obtain the bounds for each of the microscopic events at a specific confidence level ( $\alpha$ ) produces a time-dependent hyper-rectangle box  $\mathbf{m}$  formed by the extreme values of each microscopic event,  $W_n^k$ , considered in the KMC simulation, i.e.,

$$\mathbf{m}(t) = \{\mathbf{m}_1(t), \dots, \mathbf{m}_j(t), \dots, \mathbf{m}_J(t)\} : \mathbf{m}_j(t) = [W_1^k(t), \dots, W_n^k(t), \dots, W_N^k(t)] \quad (21)$$

where the block vector  $\mathbf{m}(t)$  of length  $2^N$  includes all the possible combinations between the upper and lower bounds of the  $N$  total rate of microscopic events at time  $t$ . Each element of  $\mathbf{m}$ , e.g.  $\mathbf{m}_j$ , is a vector of length  $N$  that includes a particular combination between the upper and lower limits of the  $N$  microscopic events. Similarly, the surface describing the microstructure of the system at any time  $t$  is defined as follows:

$$\mathbf{S}(t, \mathbf{m}) = \{\mathbf{S}_1(t, \mathbf{m}_1), \dots, \mathbf{S}_j(t, \mathbf{m}_j), \dots, \mathbf{S}_J(t, \mathbf{m}_J), \mathbf{S}_{nom}(t, \mathbf{m}_{nom})\} \quad (22)$$

where  $\mathbf{S}_j(t, \mathbf{m}_j)$  is a KMC lattice that represents the morphology of the surface as shown in Eq. (8), at time  $t$  due to the combination in the microscopic events' upper and lower limits specified by the vector  $\mathbf{m}_j$ . Similarly,  $\mathbf{S}_{nom}(t, \mathbf{m}_{nom})$  represents a surface describing the evolution at time  $t$  of the film using the expected values in the  $N$  microscopic events and is defined as follows:

$$\mathbf{m}_{nom}(t) = [W_1^{nom}(t), \dots, W_n^{nom}(t), \dots, W_N^{nom}(t)]$$

where  $W_n^{nom}(t)$  represents the nominal (expected) value of the  $n^{th}$  event rate at time  $t$ .

Based on the above,  $J+1$  parallel lattice-based KMC simulators, each describing the microstructure of the surface due to a particular combination in the event rates need to be simulated simultaneously to compute the lower and the upper bounds on the fine-scale properties of the system given by the KMC model outputs. Accordingly, lower and upper bounds for the thin film's key outputs at a given time  $t$  can be obtained as follows:

$$\begin{aligned} \hat{y}^{up}(t) &= \max_{\hat{y}} \hat{y}(t), \\ \hat{y}^{low}(t) &= \min_{\hat{y}} \hat{y}(t), \\ \hat{y}(t) &= [\hat{y}_1(t), \dots, \hat{y}_j(t), \dots, \hat{y}_J(t), \hat{y}_{nom}(t)] \end{aligned} \quad (23)$$

where  $\hat{y}_j(t)$  represents an output predicted from the KMC model that is calculated using properties of the microstructure of the surface  $\mathbf{S}_j(t, \mathbf{m}_j)$ . The output  $\hat{y}(t)$  can represent the roughness, growth rate or thickness of the film at a given time  $t$ , i.e.,  $r(t)$ ,  $Gr(t)$  and  $H(t)$ , respectively.

In general, the number of parallel KMC simulations depends on the number of microscopic events. Specifically for the thin film deposition process described in Section 2,  $J=2^3$  since there are three different microscopic processes occurring on the surface, i.e., adsorption, desorption and migration. Nevertheless, the sensitivities are time-varying and correspondingly the lower and upper bounds on microscopic events will change during the deposition process. When the parameter uncertainties are time-varying, propagating the uncertainty using fixed upper and lower bounds on microscopic events results in overly conservative bounds for the outputs. To alleviate this problem,  $\mathbf{S}_{nom}(t, \mathbf{m}_{nom})$  is used as the reference (nominal) surface using the nominal values of events rates. This lattice is used to update other KMC simulations, every sampling time instance,  $\Delta t$ . That is, assuming

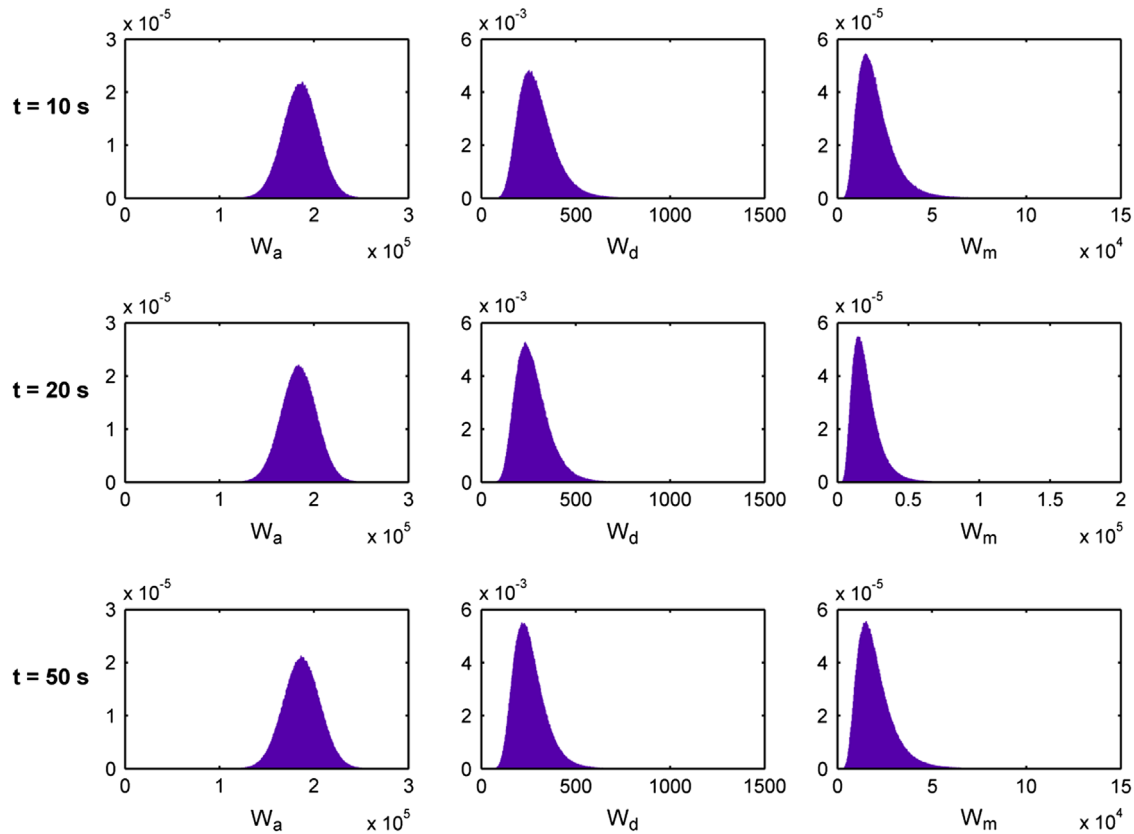


Fig. 6. Probability distribution functions obtained from power series expansion during deposition.

that the uncertain parameter is changing every  $\Delta t$  according to its probability distribution function,  $f_{p.d.}(\theta_q)$ , all the KMC lattices to be used for the next sampling interval, i.e.,  $\mathbf{S}(t + \Delta t, \mathbf{m}_j)$  are initialized with  $\mathbf{S}_{nom}(t, \mathbf{m}_{nom})$  to compute the lower and upper bounds of outputs for the next sampling time interval. This procedure continues up until the final integration time is reached. Fig. 7 summarizes the algorithm proposed in this work to determine the probabilistic-based bounds for the thin film epitaxial deposition process.

To determine the order of the PSE for each event rate, an offline, iterative approach was implemented. The commonly used algorithm starts with the first-order PSE and evaluates the approximation error using the brute-force Monte Carlo method. The algorithm iteratively increases the order of the PSE up until the error reaches to an acceptable value. This approach has also been previously suggested to determine the order of the PSE, e.g., (Nagy and Braatz, 2007, 2010). Once the algorithm converged, the resulting PSE order will be used for approximating the probability distribution of the event rates as shown in Fig. 7.

The major limitation of the proposed algorithm is its computational cost for control and optimization applications. To speed up the simulations, high-order lattices in the KMC simulations are replaced by reduced-order lattices, which also rise to other challenges. These new issues arise due to higher fluctuations encountered with smaller lattice sizes as shown in Fig. 4. To eliminate the fluctuations presented due to reduced-order lattices, the probabilistic-based bounds are estimated based on averaging the estimates obtained from multiple independent simulations.

#### 4. Robust optimization based on the probabilistic bounds

Generally, model-based optimization and control rely on the accuracy of the underlying process model used in the analysis to predict the outputs. In thin film deposition, the film microstructure is

directly shaped by the stochastic microscopic events taking place on the surface. At this level, the state of the surface can be affected by the changes in the rates of these events as a consequence of parameter uncertainty. The effect of model parameter uncertainty can result in operational conditions that are not optimal and correspondingly lead to loss in performance. Despite its importance, the proposed methodologies in the literature in multiscale optimization and control have never taken parameter uncertainty into account in their analyses. The aim of this section is to present the implementation of the probabilistic bounds framework presented in the previous section to address the robust optimization of a multiscale system under uncertainty in key operational parameters.

Surface roughness is referred to as an important film quality variable that controls the electrical and mechanical properties of micro-electronic devices. Moreover, thin film deposition process is a batch operation where a desired minimum film thickness is required to avoid an under-grown thin film at the end of the deposition process. Also, growth rate is an important factor which determines the manufacturing productivity. The key manipulated variable for this process is the substrate temperature since it affects the outputs of the system significantly. The goal in this case study is to determine the substrate temperature's time-dependent profile that optimizes the thin film properties of the model shown in Section 2 at the end of the batch process,  $t_f$ , in the presence of model parameter uncertainty, i.e.,

$$\max_{T(t)} H^{low}(t_f)$$

Subject to:  
Multiscale model, Eqs. (5)–(16)

$$r^{up}(t_f) \leq r_{max}$$

$$Gr^{low}(t_f) \geq Gr_{min}$$



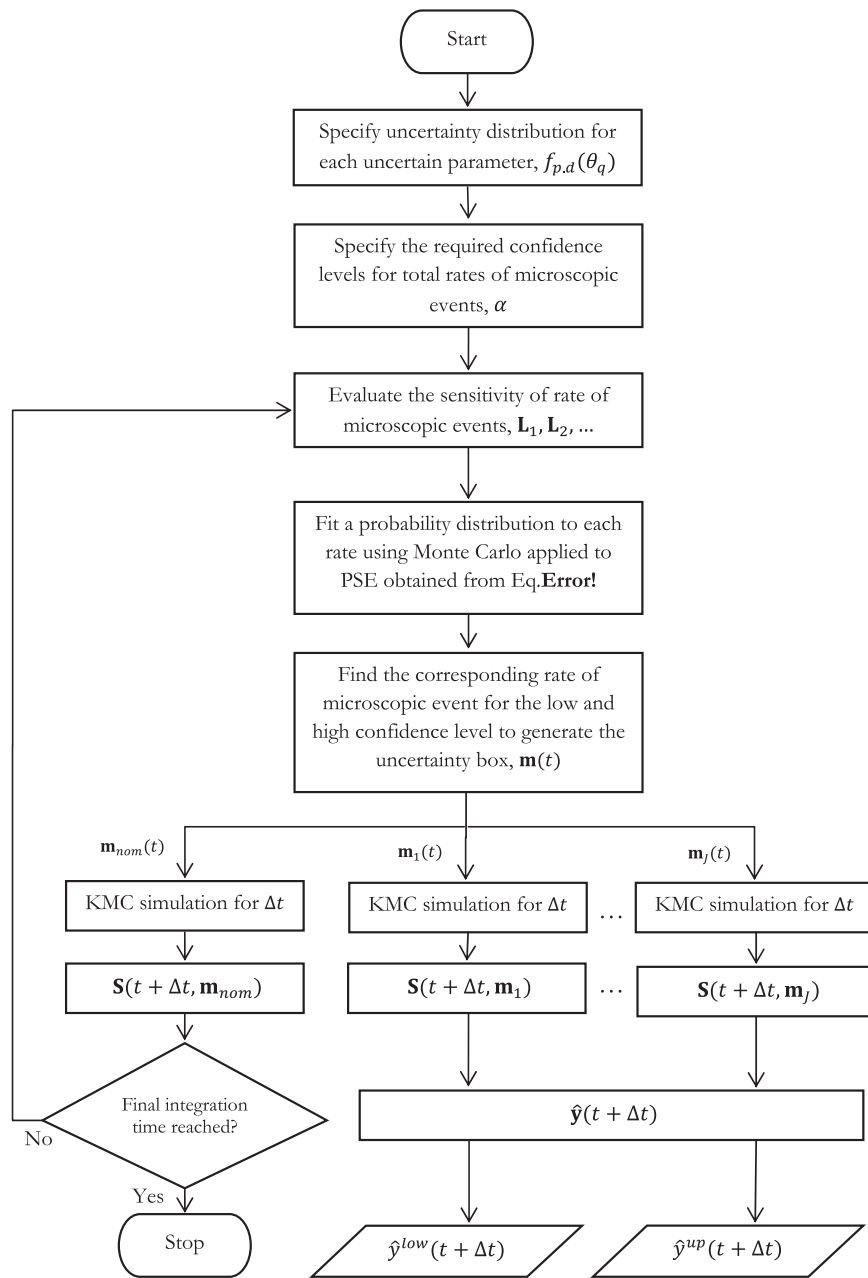


Fig. 7. Flowchart of the algorithm used to approximate the upper and lower bounds of the outputs.

$$\begin{aligned}
 &\frac{dr^{up}(t_f)}{dt} \leq \epsilon \\
 &\frac{dGr^{low}(t_f)}{dt} \leq \epsilon \\
 &T_{min} \leq T(t) \leq T_{max} \\
 &t \in [0, t_f]
 \end{aligned} \quad (24)$$

As shown above, the present optimization problem aims to maximize the lowest achievable thin film thickness at the end of the batch deposition process under uncertainty in the multiscale model's parameters. The constraint on the roughness ( $r^{up}$ ) ensures that the maximum surface roughness expected at the end of the batch is less than a maximum specification,  $r_{max}$ , whereas a minimum growth rate constraint was considered to ensure that the minimum expected growth rate at the end of the batch process ( $Gr^{low}$ ) is above a certain growth rate specification ( $Gr_{min}$ ) in the presence of uncertainty in the multiscale model parameters. The

time-dependent constraints on roughness and growth rate were added to ensure minimum variability of these parameters at the end of the batch. Following Eq. (24),  $T_{min}$  and  $T_{max}$  are respectively the minimum and maximum allowable substrate temperatures during the batch process. This problem is an infinite-dimensional nonlinear optimization problem due to the system's time-dependence. To overcome this limitation, the batch time  $t$  was discretized into a set of discrete time intervals. Accordingly, the substrate temperature trajectory,  $T(t)$ , which is the decision variable for this problem, considered the temperature at specific discrete time intervals as one of the decision variables for optimization. A piecewise constant approximation was assumed between successive temperature time intervals. At every evaluation of the optimization,  $H^{low}(t_f)$ ,  $r^{up}(t_f)$  and  $Gr^{low}(t_f)$  are determined using the probabilistic bounds method presented in the previous section. The available algorithms for parameter estimation from the experimental data mostly result in a normal

distribution (Nagy and Braatz, 2007). Accordingly, to simulate a realistic scenario, it is assumed that  $\theta = [y_b, E, E_m]$  are normally distributed uncertain parameters around their nominal values (see Table 1) with specific standard deviations.  $y_b$  is assumed as a time-invariant uncertain parameter with a standard deviation of 10% whereas  $E$  and  $E_m$  are assumed to change during operation every  $\Delta t = 1$  s with standard deviations of 3% and 5%, respectively. The bounds on the microscopic event rates were calculated at 99% confidence level. The batch time was discretized into 10 stages of  $\Delta t = 10$  s; the substrate temperature at the initial time of the batch was kept constant at  $T = 800$  K. In this study,  $r_{\max}$  and  $G_{\min}$  were set to 5.25 mL and 10.5 mL/s while  $T_{\min}$  and  $T_{\max}$  were set to 600 and 1100 K, respectively.

The optimal substrate temperature profiles for the endpoint optimization problem using only nominal values in the parameters, as well as the robust approach under parametric uncertainty are shown in Fig. 8. The optimal temperature profile obtained under parametric uncertainty demands lower temperatures at earlier stages of the deposition process to maximize the thickness as a result of high initial adsorption rates. However, close to end of the batch process, high substrate temperatures are needed to promote migration in the surface's morphology and therefore meet the constraints on roughness. Fig. 9 shows the bounds obtained using the optimal robust temperature trajectory profile. The corresponding open-loop variations of the surface roughness while using the robust temperature profile are also shown in that figure, i.e., random realizations in the uncertain parameters  $\theta$  that follow their description given above were simulated using the robust temperature profile. As shown in this figure, open-loop simulations are bounded with the upper and lower bounds obtained for roughness; the remaining constraints were also validated in the same fashion and are not shown here for brevity.

Fig. 10 shows the corresponding open-loop variations of the final surface roughness and growth rate applying 100 Monte Carlo simulations using both the nominal temperature profile and the robust optimal temperature profile. As shown in this figure, open-loop simulations employing the robust temperature profile remained within the feasible operational limits specified for this process. On the other hand, the open-loop variations of the final surface roughness applying Monte Carlo simulations using the nominal temperature profile shows that the surface roughness at the end of the batch process does not meet the specification

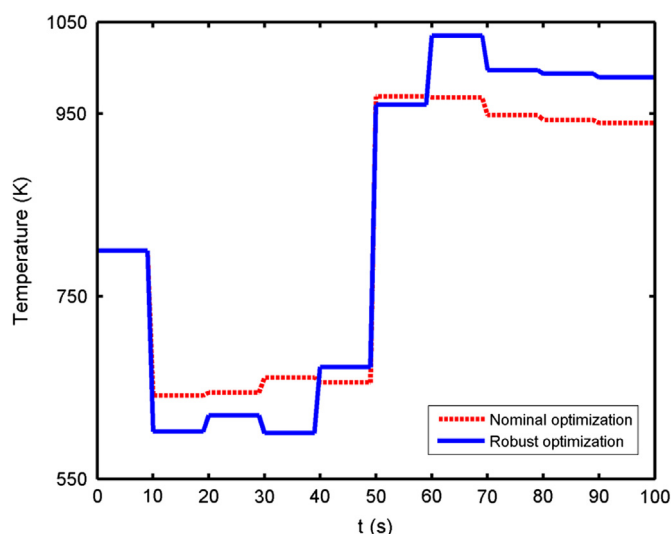


Fig. 8. Optimal temperature profile obtained using the nominal parameters and robust approach.

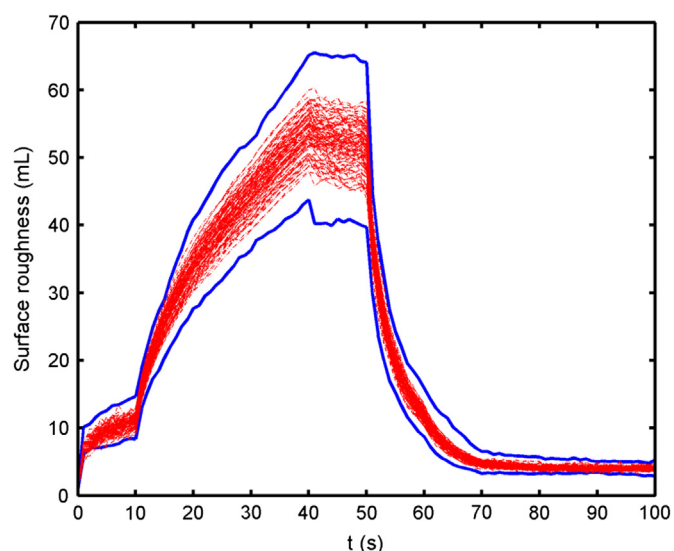


Fig. 9. The upper and lower bounds estimated for surface roughness and open-loop simulations using the robust optimal temperature profile obtained under parametric uncertainty.

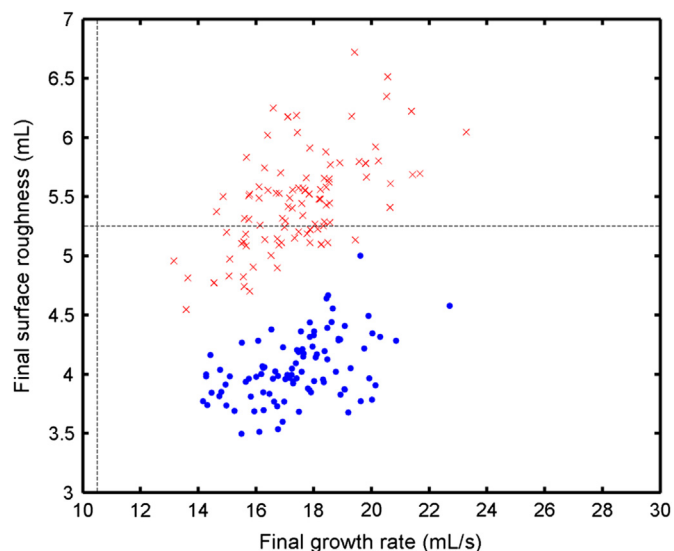


Fig. 10. Variation of final properties due to parameter uncertainties, obtained from the open-loop simulations applying various temperature profiles. The dashed lines are the constraint on the final surface roughness and growth rate; the dots are for the robust temperature profile while the x-marks are for the nominal temperature profile.

considered for this variable ( $r_{\max}$ ) most of the time, which results in a loss in performance.

## 5. Conclusions

The main contribution of this paper is to employ higher order PSEs for uncertainty analysis of multiscale systems. Although series expansions have been employed in the literature for sensitivity analysis of multiscale systems, this paper employs PSEs for robust optimization of multiscale systems under uncertainty. A systematic framework to analyze the model uncertainty propagation based on the PSE was explored. To describe the thin film growth process, a multiscale model is simulated linking continuum conservation laws, describing the macro-scale phenomena, with a lattice-based KMC simulator, which describes the film's

growth evolution on the surface. The uncertainty in the parameters of the KMC simulations and in the boundary condition of the mass transfer equation is propagated into total rates of microscopic events using power series expansions. That is, having the prior distribution of the uncertain parameters and estimating the sensitivities, the probability distribution of microscopic events are determined using the PSE-based models. Subsequently, upper and lower bounds on the outputs are estimated using the events distributions. The computational feasibility for robust optimization is achieved using multiple reduced-order lattices in KMC simulator. The method is used to obtain the optimal substrate temperature trajectory that maximizes the endpoint thin film thickness while meeting constraints on the roughness and growth rate in the presence of uncertainty in the multiscale model's parameters. The proposed approach is evaluated through simulations that show that the system's outputs remained within their corresponding feasible operational limits under uncertainty. Although the proposed method is applied for open-loop optimization of thin film deposition process, it has significant potential for closed-loop purposes. Therefore, the present approach is a practical efficient tool that can be used to address the robust control and optimization of multiscale systems under parametric uncertainty.

## Acknowledgements

The authors would like to acknowledge the financial support provided by the Natural Sciences and Engineering Research Council of Canada (NSERC).

## References

- Albo, S.E., Broadbelt, L.J., Snurr, R.Q., 2006. Multiscale modeling of transport and residence times in nanostructured membranes. *AIChE J.* 52, 3679–3687.
- Braatz, R.D., Alkire, R.C., Rusli, E., Drews, T.O., 2004. Multiscale systems engineering with applications to chemical reaction processes. *Chem. Eng. Sci.* 59, 5623–5628.
- Braatz, R.D., et al., 2006. Perspectives on the design and control of multiscale systems. *J. Process Control* 16, 193–204.
- Christofides, P.D., Armaou, A., 2006. Control and optimization of multiscale process systems. *Computers & Chem. Eng.* 30, 1670–1686.
- Christofides, P.D., Armaou, A., Lou, Y., Varshney, A., 2008. Control and optimization of multiscale process systems. Birkhäuser, Boston.
- Dollet, A., 2004. Multiscale modeling of CVD film growth—a review of recent works. *Surf. Coat Technol.* 177, 245–251.
- Drews, T.O., Braatz, R.D., Alkire, R.C., 2003. Parameter sensitivity analysis of Monte Carlo simulations of copper electrodeposition with multiple additives. *J. Electrochem. Soc.* 150, C807–C812.
- Fichthorn, K.A., Weinberg, W.H., 1991. Theoretical foundations of dynamical Monte Carlo simulations. *J. Chem. Phys.* 95, 1090–1096.
- Gadgil, P.N., 1993. Single wafer processing in stagnation point flow CVD reactor: prospects, constraints and reactor design. *J. Electronic. Mater.* 22, 171–177.
- Gallivan, M.A., 2003. Optimization, estimation, and control for kinetic Monte Carlo simulations of thin film deposition. Piscataway, New Jersey, USA. In: Proceedings of the Conference on Decision and Control, IEEE Press, pp. 3437–3442.
- Gallivan, M.A., 2005. An estimation study for control of a lattice model of thin film deposition. *Comput. Chem. Eng.* 29, 761–769.
- Gallivan, M.A., Atwater, H.A., 2004. Design of a film surface roughness-minimizing molecular beam epitaxy process by reduced-order modeling of epitaxial growth. *J. Appl. Phys.* 95, 483–489.
- Gallivan, M.A., Murray, R.M., 2004. Reduction and identification methods for Markovian control systems, with application to thin film deposition. *Int. J. Robust Nonlinear Control* 14, 113–132.
- Gilmer, G.H., Bennema, P., 1972. Simulation of crystal growth with surface diffusion. *J. Appl. Phys.* 43, 1347–1360.
- Hu, G., Orkoulas, G., Christofides, P.D., 2009. Regulation of film thickness, surface roughness and porosity in thin film growth using. *Chem. Eng. Sci.* 64, 3903–3913.
- Lam, R., Vlachos, D.G., 2001. Multiscale model for epitaxial growth of films: growth mode transition. *Phys. Rev. B* 64, 035401.
- Lou, Y., Christofides, P.D., 2003a. Estimation and control of surface roughness in thin film growth using kinetic Monte-Carlo models. *Chem. Eng. Sci.* 58, 3115–3129.
- Lou, Y., Christofides, P.D., 2003b. Feedback control of growth rate and surface roughness in thin film growth. *AIChE J.* 49, 2099–2113.
- Lou, Y., Christofides, P.D., 2004. Feedback control of surface roughness of GaAs (001) thin films using kinetic Monte Carlo models. *Comput. Chem. Eng.* 29, 225–241.
- Ma, D.L., Braatz, R.D., 2001. Worst-case analysis of finite-time control policies. *IEEE Trans. Control Syst. Technol.* 9, 766–774.
- Majumder, D., Broadbelt, L.J., 2006. A multiscale scheme for modeling catalytic flow reactors. *AIChE J.* 52, 4214–4228.
- Middlebrook, S.A., Rawlings, J.B., 2006. State estimation approach for determining composition and growth rate of  $\text{Si}_{1-x}\text{Ge}_x$  chemical vapor deposition utilizing real-time ellipsometric measurements. *Appl. Opt.* 45, 7043–7055.
- Middlebrooks, S.A., Rawlings, J.B., 2007. Model predictive control of  $\text{Si}_{1-x}\text{Ge}_x$  thin film chemical-vapor deposition. *IEEE Trans. Semicond. Manuf.* 20, 114–125.
- Nagy, Z.K., Allgower, F., 2007. A nonlinear model predictive control approach for robust end-point property control of a thin-film deposition process. *Int. J. Robust Nonlinear Control* 17, 1600–1613.
- Nagy, Z.K., Braatz, R.D., 2003. Worst-case and distributional robustness analysis of finite-time control trajectories for nonlinear distributed parameter systems. *IEEE Trans. Control Syst. Technol.* 11, 694–704.
- Nagy, Z.K., Braatz, R.D., 2004. Open-loop and closed-loop robust optimal control of batch processes using distributional and worst-case analysis. *J. Process Control* 14, 411–422.
- Nagy, Z.K., Braatz, R.D., 2007. Distributional uncertainty analysis using power series and polynomial chaos expansions. *J. Process Control* 17, 229–240.
- Nagy, Z.K., Braatz, R.D., 2010. Distributional uncertainty analysis using polynomial chaos expansions. In: Proceedings of the IEEE International Symposium on Computer-Aided Control System Design. Yokohama, Japan.
- Ni, D., Christofides, P.D., 2005. Multivariable predictive control of thin film deposition using a stochastic PDE model. *Ind. Eng. Chem. Res.* 44, 2416–2427.
- Prasad, V., Vlachos, D.G., 2008. Multiscale model and informatics-based optimal design of experiments: application to the catalytic decomposition of ammonia on ruthenium. *Ind. Eng. Chem. Res.* 47, 6555–6567.
- Raimondeau, S., Aghalayam, P., Mhadeshwar, A.B., Vlachos, D.G., 2003. Parameter optimization of molecular models: application to surface kinetics. *Ind. Eng. Chem. Res.* 42, 1174–1183.
- Raimondeau, S., Vlachos, D.G., 2000. Low-dimensional approximations of multiscale epitaxial growth models for microstructure control of materials. *J. Comput. Phys.* 160, 564–576.
- Ricardez-Sandoval, L.A., 2011. Current challenges in the design and control of multiscale systems. *Can. J. Chem. Eng.* 89, 1324–1341.
- Rusli, E., Drews, T.O., Braatz, R.D., 2004. Systems analysis and design of numerically coupled multiscale reactor simulation codes. *Chem. Eng. Sci.* 59, 5607–5613.
- Rusli, E., Feng, X., Drews, T.O., Vereecken, P.M., Andricacos, P., Deligianni, H., Braatz, R.D., Alkire, R.C., 2007. Effect of additives on shape evolution during electrodeposition II. Parameter estimation from roughness evolution experiments. *J. Electrochem. Soc.* 154, D584–D597.
- Sharma, O.P., Sirignano, W.A., 1969. Ignition of stagnation point flow by a hot body. *Combust. Sci. Technol.* 1, 95–104.
- Song, X., Williams, W.R., Schmidt, L.D., Aris, R., 1991. Bifurcation behavior in homogeneous-heterogeneous combustion: II. computations for stagnation-point flow. *Comb. Flame* 84, 292–311.
- Subramanian, K., Kumar, S., Patwardhan, S.C., Prasad, V., 2011. Extensions to experiment design and identification algorithms for large-scale and stochastic processes. *Int. J. Adv. Mechatron. Syst.* 3, 3–13.
- Van Kampen, N.G., 1992. Stochastic processes in physics and chemistry. North-Holland, Amsterdam.
- Varshney, A., Armaou, A., 2005. Multiscale optimization using hybrid PDE/kMC process systems with application to thin film growth. *Chem. Eng. Sci.* 60, 6780–6794.
- Varshney, A. & Armaou, A., 2006. Feedback control of surface roughness during thin-film growth using approximate low-order ODE model. In: Proceedings of the 45th IEEE Conference on Decision and Control, IEEE Press, San Diego, CA, USA, pp. 4413–4418.
- Vlachos, D.G., 1997. Multiscale integration hybrid algorithms for homogeneous-heterogeneous reactors. *AIChE J.* 43, 3031–3041.
- Vlachos, D.G., 1999. The role of macroscopic transport phenomena in film microstructure during epitaxial growth. *Appl. Phys. Lett.* 74, 2797–2799.
- Vlachos, D.G., 2005. A review of multiscale analysis: examples from systems biology, materials engineering, and other fluid-surface interacting systems. *Adv. Chem. Eng.* 30, 1–61.
- Vlachos, D.G., 2012. Multiscale modeling for emergent behavior, complexity, and combinatorial explosion. *AIChE J.* 58, 1314–1325.
- Yang, A., 2013. On the common conceptual and computational frameworks for multiscale modeling. *Ind. Eng. Chem. Res.* 52, 11451–11462.
- Zhang, X., Hu, G., Orkoulas, G., Christofides, P.D., 2010. Predictive control of surface mean slope and roughness in a thin film deposition process. *Chem. Eng. Sci.* 65, 4720–4731.